The 6th International Symposium on Transport Phenomena in Thermal Engineering
May 9-13, 1993, Seoul, Korea

SURFACE RADIATION EXCHANGE IN MULTI-DIMENSIONAL ARRAYS OF ELECTRONIC COMPONENTS

A. Sanchez A.,[1] Ramiro Bravo,[2] Theodore F. Smith[3]

[1]*Universidad de los Andes, Escuela de Ingeniería Mecánica, Mérida, Edo. Mérida 5101, VENEZUELA*
[2]*Department of Mechanical and Aerospace Engineering, Tri-State University, Angola, Indiana, 46703-0307, USA*
[3]*Department of Mechanical Engineering, College of Engineering, The University of Iowa, Iowa City, Iowa 52242, USA*

1. ABSTRACT

In the present paper, the discrete ordinates method is used to simulate the thermal performance of 2-D and 3-D arrays of electronic components. The simulations include pure radiation as well as combined mechanisms of radiation and convection.

It is corroborated in the paper that in 2-D situations, and with air as the cooling medium, the best simulations are obtained when an equally spaced quadrature is used. Although no effort is made in the paper to minimize end effects in the 3-D geometries, experimental estimates with the level-odd symmetric quadrature indicate that the contribution of radiative transfer to the total heat transfer process is of the order of 33%.

2. INTRODUCTION

In recent years, the development of more powerful and more compact electronic equipment has resulted in the need for more and better cooling techniques. Of paramount importance in the development of these techniques are the predictions, based on numerical simulations, of the heat transfer mechanisms associated with the electronic components of the equipment.

Fig. 1 shows a common setup for electronic components. In this configuration, the heat dissipating elements are mounted on a board and separated from the rest of the equipment by an upper wall creating a passage where the cooling fluid circulates. The heat transfer from the array to the surroundings takes place by convection to the cooling medium, conduction to the mounting board, and radiation exchange among all the surfaces.

There are several studies where the convective effects have been analyzed in both 2- and 3-D geometries (Sparrow, et. al., 1982; Braaten and Patankar, 1985; Jaluria, 1985; Asako and Faghri, 1988; Afrid and Zebib, 1989; Shaw, et. al, 1991). Work considering combined radiation/convection effects are less common (Lee and Yovanovich, 1989; Smith, et al., 1991; Bravo, et al., 1992).

In the present work, attention is focused on the radiative effects and in the procedure needed to include these effects in conjugate heat transfer calculations. In particular, the discrete ordinates method is used to evaluate the radiative transfer equations in 2- and 3-D applications. The applicability of the method is exemplified by three examples that include pure radiation in 2- and 3-D settings and combined radiation/forced convection in the 3-D geometry shown in Fig. 1.

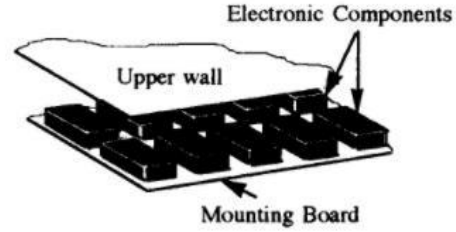

Figure 1.Schematic Diagram of General Geometry

3. ANALYSIS

3.1. System Description

Fig. 1 shows a general configuration of electronic components where the designer would like to evaluate the heat exchange rate between the different surfaces as well as to specify the spatial distribution of this heat exchange, in order to formulate, properly, the cooling requirements of the system. Radiation heat transfer accounts for a good part of the total energy exchanged in this geometry. To evaluate this exchange of radiant energy by means of traditional view factors, or cross string methods can be, in a configuration like the one depicted in Fig. 1, extremely tedious if not impossible. If the electronic modules are of different shapes and dimensions, the problem is practically intractable. The discrete ordinates method, on the other hand, offers the possibility of solving these types of problems with relative ease.

A cooling fluid could circulate between the plates in order to provide a cooling effect due to convection. For the present work, and independently of the inclusion or not of convective heat transfer, the fluid between the plates is considered to be air.

3.2. Governing Ecuations

Radiative transfer. The radiative transfer algorithm used in this study (ANDISORD4, Sánchez, et al., 1992) is based on the discrete ordinates model, and it has built in the possibility of solving for non-homogeneous media. The system described here (air-modules) is treated as a non-homogeneous problem with two components, air and solid. The only difference between a solid component (protrusion) and any other gaseous component, in a multi-component system, is the presence, in the former, of internal boundaries. As a consequence ANDISORD4 requires the user to specify for the solid components, as it would for any other boundary, the emittance and transmittance.

The propagation of radiation (I) along a line-of-sight direction ζ is described by the radiative transfer equation. Without scattering, the change in the radiant intensity $I(\zeta)$ in the $\bar{\omega}$-direction is expressed by

$$\frac{dI}{d\zeta} = - \beta\, I(\zeta) + a\, I_b \qquad (1)$$

In Eq. (1), β is the extinction coefficient given by the sum of the absorption coefficient (a) and scattering coefficient (s). Eq. (1) is subject to the following boundary conditions

$$I^+ = \varepsilon\, I_b^+ + \frac{\rho_d}{\pi} f_d \int_0^{2\pi} (I^-(\bar{\omega}_i)\, \eta\, d\omega^-) + \rho_d\,(1 - f_d)\, I_m^- \qquad (2)$$

In Eq. (2), superscripts + and - indicate radiation going from the boundary toward the medium inside the domain, and from the medium toward the boundary, respectively. The boundary has an emittance ε and blackbody intensity I_b^+ which depends on the temperature of the surface. The reflectance of the boundary is denoted by ρ_d, which, for convenience, is taken to be independent of direction. The fraction of the reflection that is diffuse is f_d. The cosine of the angle between the direction of propagation of I^- and the normal to the given boundary is η. The intensity in the direction mirroring the direction of I^+, that is, the specularly reflected intensity, is I_m^-. Physically, the terms on the right-hand-side of Eq. (2) represent emission, diffuse reflection of incident intensity from within the medium, and specular reflection of incident intensity. The expression in Eq. (2) could be modified to account for bidirectional reflectance and transmittance distribution functions. The intensities of I_b^+, and I_{ba}^o are assumed known.

The divergence of the radiative flux is expressed as

$$\nabla\cdot\bar{q}_r = a\,\pi\, I_b - a \int_0^{4\pi} I_\lambda(\bar{\omega})\, d\omega \qquad (3)$$

where a is the monochromatic absorption coefficient, I_b is the monochromatic blackbody intensity evaluated using Planck's law, I is the radiant intensity for the $\bar{\omega}$-direction, and ω is the solid angle. The dependency of a, I_b, and I on the spatial variables is understood.

Transport equations. For laminar flow and steady-state conditions with all the properties of the fluid assumed constant except for the density related to the buoyancy effect (Boussinesq approximation in the y momentum equation), the transport equations for 3-D flow are:

Continuity:

$$\frac{\partial}{\partial x}(\rho\, u) + \frac{\partial}{\partial y}(\rho\, v) + \frac{\partial}{\partial z}(\rho\, w) = 0 \qquad (4)$$

x-momentum:

$$\frac{\partial}{\partial x}(\rho\, u\, u) + \frac{\partial}{\partial y}(\rho\, u\, v) + \frac{\partial}{\partial z}(\rho\, u\, w) = \frac{\partial}{\partial x}\left(\mu_f \frac{\partial u}{\partial x}\right) + \frac{\partial}{\partial y}\left(\mu_f \frac{\partial u}{\partial y}\right) + \frac{\partial}{\partial z}\left(\mu_f \frac{\partial u}{\partial z}\right) - \frac{\partial P}{\partial x} \qquad (5)$$

y-momentum:

$$\frac{\partial}{\partial x}(\rho\, v\, u) + \frac{\partial}{\partial y}(\rho\, v\, v) + \frac{\partial}{\partial z}(\rho\, v\, w) = \frac{\partial}{\partial x}\left(\mu_f \frac{\partial v}{\partial x}\right) + \frac{\partial}{\partial y}\left(\mu_f \frac{\partial v}{\partial y}\right) + \frac{\partial}{\partial z}\left(\mu_f \frac{\partial v}{\partial z}\right) - \frac{\partial P}{\partial y} + \rho\, \underline{g}\, \beta_e\, (T - T_c) \qquad (6)$$

z-momentum:

$$\frac{\partial}{\partial x}(\rho\, w\, u) + \frac{\partial}{\partial y}(\rho\, w\, v) + \frac{\partial}{\partial z}(\rho\, w\, w) = \frac{\partial}{\partial x}\left(\mu_f \frac{\partial w}{\partial x}\right) + \frac{\partial}{\partial y}\left(\mu_f \frac{\partial w}{\partial y}\right) + \frac{\partial}{\partial z}\left(\mu_f \frac{\partial w}{\partial z}\right) - \frac{\partial P}{\partial z} \qquad (7)$$

energy:

$$\rho C_p \frac{DT}{Dt} = \beta_e T \frac{DP}{Dt} + \nabla\cdot(k\, \nabla T - \bar{q}_r) \qquad (8)$$

In the previous equations ρ is the density; u,v,and w are the velocity components with x, y, and z respectively; μ_f is the viscosity of the fluid; P, $\underline{g}$, and β_e are pressure, gravity, and expansion coefficient respectively; T is temperature; and k is the thermal conductivity.

The transport equations and the energy equation were solved using the program FANS-3D (Bravo, 1991) which is based on the finite analytic method (Chen, 1988).

4. EXAMPLES

4.1. Example 1: Pure Radiation in a 2-D System

For this first example, the dimensions, disposition, and grid discretization are shown in Fig. 2. The board, the components, and the other walls are considered to be isothermal surfaces at 310 K, 320 K, and 300 K respectively.

Two different cases were solved. In the first case, all the participating surfaces are considered to be black. In the second case, on the other hand, the board, the components, and the other walls have emissivities of 0.9, 0.8, and 0.5 respectively.

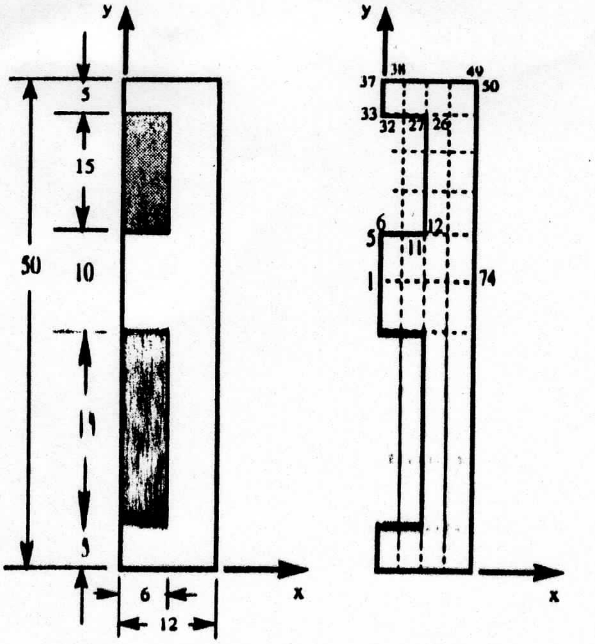

a) Dimensions in mm b) Surface Grid Location

Figure 2. Schematic Diagram of 2-D Enclosure

The discrete ordinates method requires the selection of a quadrature set and the definition of a finite-difference interpolating factor (α). After experimenting with several quadrature sets (Fiveland, 1991), a set based on equal weights and equal angular increments of the polar angle was found to be more accurate for the calculation of heat fluxes. This choice of an equally spaced, equally weighted quadrature set for 2-D problems with transparent medium had been previously suggested by Sánchez and Smith, 1992, where more information can be found.

Heat transfer fluxes evaluated with the discrete ordinates method (ANDISORD4) where compared with exact values based on the radiosity/irradiation method (Sparrow and Cess, 1978; Sánchez and Smith, 1992) referred here after as RIM. Results of these comparisons are shown in Fig. 3 where MG denotes the number of discrete directions per quadrant, and ALFA (α) indicates the finite-difference interpolating factor needed in the discrete ordinates calculations. Values of MG grater than 15 did not produce in any significant improvement in the results. The optimun value for α was found to be around 0.52 for the black case and 0.55 for the gray one. The value of α = 0.6 was selected, however, for consistency with previous studies (Sánchez and Smith, 1992) where α = 0.6 has been suggested as a standard for 2-D problems with non-participating medium.

The main difficulty of this example arises from the sharp discontinuities and from the non-participating characteristic of the medium. It can be seen in Fig. 3 that, with the recommended quadrature and interpolating factor, the value of the heat transfer fluxes evaluated with the discrete ordinates method (ANDISORD4) closely match those evaluated with the RIM method.

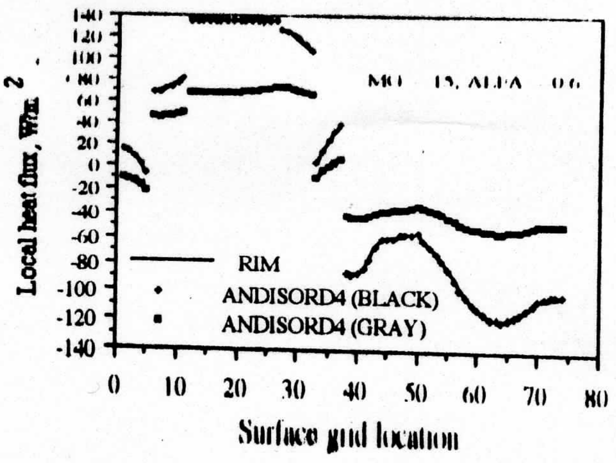

Figure 3 Local heat fluxes for black and gray surfaces

4.2. Example 2: Pure Radiation in a 3-D System

Consider an infinite array of electronic components as the one sketched in Fig. 1. The top and bottom walls are maintained at constant temperatures of 300 K and 310 K respectively while the electronic components are kept at a constant temperature of 320 K. The medium is a non participating gas (air) and the dimensions and relative position of the components are represented in Fig. 4, where Sp and Sc are 3.3 cm and 2.4 cm respectively. For this particular exercise, the modules, as well as the top and bottom surfaces, are considered radiatively black.

In the infinite array of electronic components, object of this problem, the radiation field is periodic. Further, the resulting periodic, imaginary surfaces (boundaries of the "numerical domain" in Fig. 4) are also symmetric. ANDISORD4 has the capabilities built in for taking advantage of this symmetry and/or periodicity. The physical domain of the problem becomes drastically reduced when this capability is used. For the particular problem being solved here, the numerical domain indicated in Fig. 4 was used (notice that even half of this domain –in the z direction– could have been used as the numerical domain) and the bounding surfaces were declared as planes of symmetry (for this problem the bounding surfaces could have been declared periodic boundaries with no change in the results).

For the solution of this problem, the discrete ordinates model was implemented with a S-6 LSO quadrature set (Fiveland, 1991) on an 11x7x22 grid mesh. The wall clock time needed to reach the final solution was 15 minutes. The symmetry of the fluxes is easily observed in Fig. 5 and 6. It was verified that the heat fluxes at all the symmetric planes were zero and that energy was conserved. Fig. 5 and 6 show the calculated heat fluxes through the top and bottom surfaces respectively. The initial values of 0.07 for both x and z, correspond to the first grid element in the computational domain.

4.3. Example 3: Radiation/Forced Convection in a Three-Dimensional System

In this example, the combined effect of convection and radiation heat transfer is studied in the array of electronic chips displayed in Fig. 1. The modules are cooled by a radiatively non-participating gas (air) flowing inside the passage. This is an important problem in the design of electronic equipment that has been previously studied, without the inclusion of radiation, using different techniques and approximations (Shaw, et al., 1991; Asako and Faghri, 1988; Braaten and Patankar, 1985; Sparrow, et al., 1982).

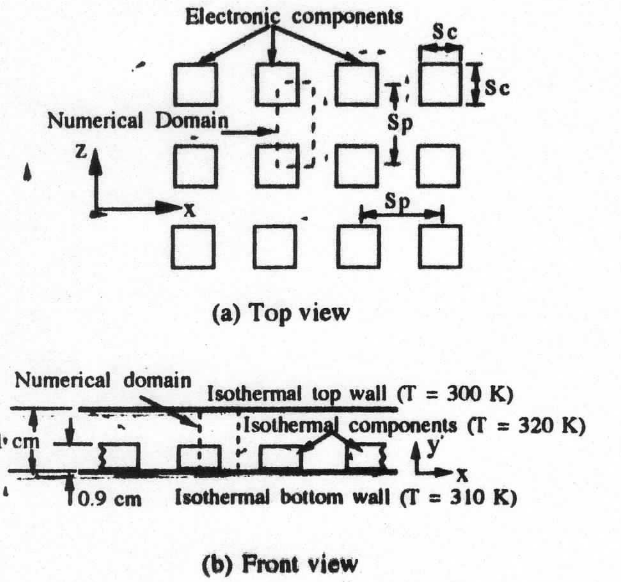

Figure 4. Top and front view for the geometry in Example 2.

To simplify the solution of the problem, fully developed periodic flow, as discussed in Bravo, et al., 1992, is assumed. Defining a dimensionless temperature:

$$\theta_t(x,y,z) = \frac{T(x,y,z) - T_{ref}}{T_{bz} - T_{ref}} \qquad (9)$$

where $T(x,y,z)$ is the temperature at any location (x,y,z), T_{ref} is a reference temperature, and T_{bz} is the bulk temperature defined at location z by:

$$T_{bz} = \frac{\int_A T(x,y,z)\ |w|\ dA}{\int_A |w|\ dA} \qquad (10)$$

and A is the area of the cross section at z and w is the velocity normal to that area.

More convenient to use than the dimensionless temperature given in Eq. 9 is:

$$\phi_t(x,y,z) = \frac{T(x,y,z) - T_{ref}}{T_{bi} - T_{ref}} \qquad (11)$$

which is expressed in terms of the inlet bulk temperature.

For a given domain, the assumption of periodicity implies that the velocity field and the dimensionless temperature (θ_t) repeat themselves at specific equal distances (numerical domain) along the direction of the flow. The periodic condition on the dimensional temperature field between inlet and outlet of the numerical domain ($\theta_{ti} = \theta_{to}$) can be expressed as:

$$T_i = T_{ref} + (T_o - T_{ref}) \frac{T_{bi} - T_{ref}}{T_{bo} - T_{ref}} \qquad (12)$$

or, in terms of ϕ

$$\phi_{ti} = \phi_{to} \frac{T_{bi} - T_{ref}}{T_{bo} - T_{ref}} \qquad (13)$$

where subscripts i and o indicate inlet and outlet respectively.

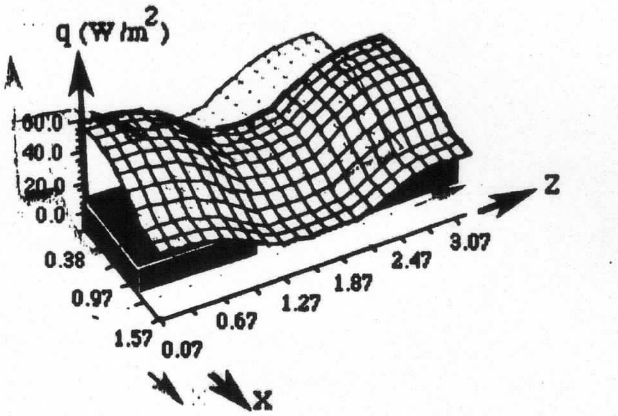

Figure 5. Heat flux through the top wall for Example 2

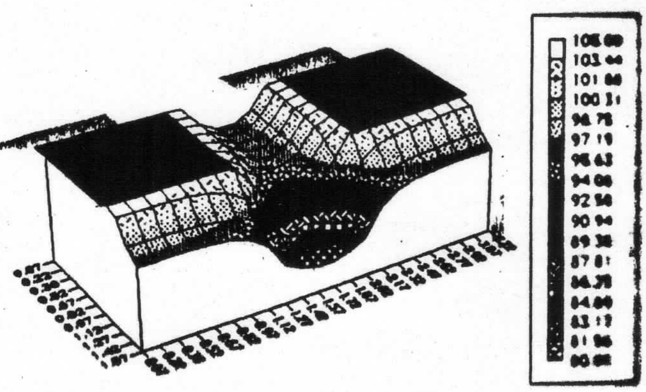

Figure 6. Heat flux through the bottom wall for Example 2. (W/m²)

In particular, for this problem, periodicity and symmetry reduce the domain to the element represented in Fig. 7. The fluid flow, considered laminar (Re = 100.0 based on the periodic length of the domain along the z axis), is in the positive z direction.

The top view for this problem is equivalent to the top view shown in Fig. 4 for Example 2 with Sp and Sc being 3.6 cm and 2.4 cm respectively. For the numerical domain shown in Fig. 7, the planes at x=0.0 and at x=1.5 cm are considered planes of symmetry; the planes at the fluid inlet and outlet are periodic; and the top and bottom walls are adiabatic. The inlet temperature of the fluid is considered equal to 305 K and the temperature of the blocks (used as reference temperature in Eq. 10 and Eq. 11) is constant and equal to 320 K. All surfaces are assumed black.

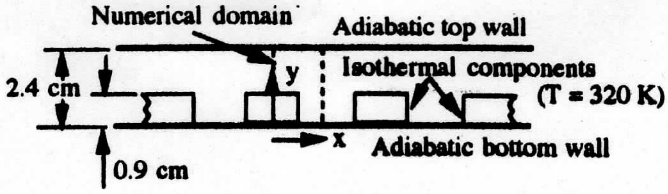

Figure 7. Geometry for Example 3 (Front view).

The problem was solved on a non-uniform 15x20x30 grid mesh. This grid is set by the fluid flow program, and ANDISORD4 adapts to it. Because the Navier-Stokes equations and the energy equation are decoupled, FANS-3D solved the problem, initially, for the velocity field. Some of the results are shown in Fig. 8 where the velocity profiles for the flow component in the z direction are displayed at two locations, at the inlet and at the center between the blocks (for more detailed results on the velocity field see Bravo, et al., 1992).

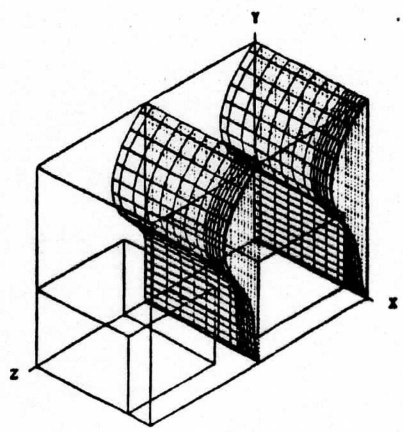

Figure 8. Profiles of the velocity component in the z direction for Example 3.

Because the medium is non-participating, the divergence of the radiative heat flux vector in the energy equation vanishes and the transport and radiation models become explicitly decoupled. With the velocity field known, the energy equation is solved by FANS-3D to obtain convection-alone temperature distributions. The results obtained (in terms of ϕ) are shown in Fig. 9(a).

From the definition of ϕ, the dimensionless temperature on the blocks is zero. It is clearly appreciated in Fig. 9(a) that, as expected, the temperature profiles are perpendicular to the top and bottom insulated plates. In this figure we can also appreciate that the fluid moving between the blocks reaches a temperature close to that of the modules, particularly in the region close to the bottom wall. The maximum dimensionless temperature ϕ (coldest dimensional temperature) is on the top insulated wall. To procure these solutions, the boundar conditions of adiabatic top and bottom walls; symmetric latera "walls"; and periodic inlet and outlet are used:

$$\text{at } y = 0.0 \text{ and } y = 2.4 \text{ cm} \qquad \frac{\partial \theta}{\partial y} = 0.0 \quad \text{(adiabatic)} \qquad (14$$

$$\text{at } x = 0.0 \text{ and } x = 1.5 \text{ cm} \qquad \frac{\partial \theta}{\partial x} = 0.0 \quad \text{(symmetric)} \qquad (15$$

$$\text{at } z = 0.0 \text{ and } z = 3.0 \text{ cm} \qquad \theta_{ti} = \theta_{to} \qquad (16$$

With the convection-alone temperature field known ANDISORD4 is used. The radiation field is assumed to b periodic in the z direction and the planes at x = 0.0 and x = 1.: cm are symmetric. From the grid and temperature information received from FANS-3D, ANDISORD4 calculates and returns to the host program (FANS-3D) the heat fluxes at all the solid boundaries based on a S-8 LSC quadrature set (Fiveland, 1991) implementation. Although the heat flux divergences are also evaluated at every grid element the non-participating nature of the medium in this problem renders these sources equal to zero. New wall temperatures, at any location (x,y,z) are calculated through energy balances on the walls ($q_{radiation} = q_{convection}$ at the wall) resulting in:

$$T_w = T_{fl} - q_r \frac{\Delta L}{k} \qquad (17)$$

where T_w is the wall temperature, T_{fl} is the temperature of the fluid for the node adjacent to the wall, ΔL is the distance between the center of that node and the wall, q_r is the radiative heat flux (positive if it is going from the wall to the fluid and negative if it is going from the fluid to the wall), and k is the thermal conductivity of the air taken as $26.3 \cdot 10^{-3}$ W/m K.

The newly calculated wall temperatures are now used as boundary conditions by FANS-3D to evaluate new fluid temperatures. ANDISORD4 is called again, and the iteration process is repeated. The numerical procedure is considered converged when, after two iterations, the wall temperatures calculated from Eq. 17 do not change by more than a given epsilon. The final dimensionless temperature distribution (ϕ) for this problem (including radiation) is presented in Fig. 9(b). The temperature profiles are quite different from the ones previously discussed for convection alone. Typical S curves appear, and the maximum value of ϕ (coldest dimensional temperature) is now displaced to the central region between the top plate and the blocks. This effect can be better appreciated in the lateral view shown in Fig. 9(b). It is also seen in this figure that the top and bottom surfaces have increased their temperatures as a consequence of radiation being considered. The radiation arriving or leaving any one of the insulated boundaries is balanced with the heating or cooling due to convection at the surface. This results in the positive slope exhibited by the temperature profile near the insulated top boundaries that is indicative of the heat transfer, by convection, from the wall to the fluid. On the other hand, the slope of the ϕ profile close to the bottom plate indicates that heat is being transfered, by convection, from the fluid to the bottom wall.

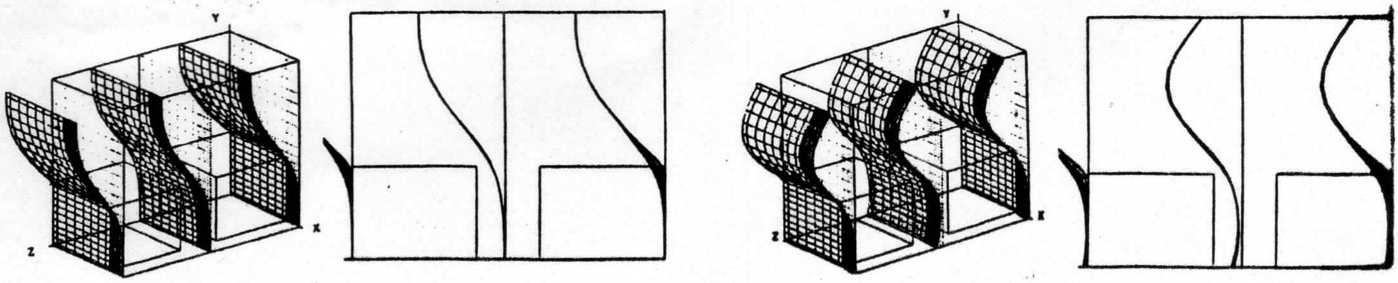

(a) Convection Alone (b) Convection + Radiation

Figure 9. Dimensionless temperature Profiles

5. CONCLUSIONS

In this paper, the discrete ordinates method has been successfully applied to three different problems related to the cooling needs of electronic components in the presence of non-participating medium.

For two-dimensional applications (Example 1) it was corroborated that the use of an equally spaced, equally weighted quadrature set and the choice of the a finite-difference factor of 0.6 produce results that are comparable to exact ones.

For three-dimensional problems where radiation alone is considered (Example 2) it was shown that the direct application of the discrete ordinates model produced results that are qualitatively plausible with conserved symmetry and energy.

When radiation is included in the forced convection calculations of Example 3, the heat transfer rate is 33 % higher than the heat transfer rate when only convection is considered. This latest result is illustrative of the importance of considering radiative heat transfer when designing the cooling needs of electronic components.

It should be noticed that the non-participating nature of the medium in these examples is not a consequence of any type of limitation of the discrete ordinates model used here, but rather a condition of this type of problems where the cooling fluid is normally air. It should also be understood that the non-participating nature of the medium will result in ray effects. The results presented here, therefore, are good approximations, but not exact results. To mitigate ray effects in 3-D problems, a higher order of quadrature and/or finer grid might be needed.

Finally, it should be mentioned that the problem of finding an optimum quadrature set for 3-D problems in the presence of non-participating medium remains an open problem.

REFERENCES

Afrid, M., & Zebib, A., 1989, Natural Convection Air Cooling of Heated Components Mounted on a Vertical Wall, Numerical Heat Transfer, Part A, Vol. 15, pp. 243-259.

Asako, Y., & Faghri, M., 1988, Three-Dimensional Heat Transfer in a Fluid Flow Analysis of Arrays of Square Blocks Encountered in Electronic Equipment, Numerical Heat Transfer, Vol. 13, pp. 481-[illegible]

Braaten, M. E., & Patankar, S. V., 1985, Analysis of Laminar Mixed Convection in Shrouded Arrays of Heated Rectangular Blocks, Int. J. Heat and Mass Transfer, Vol. 28, No. 9, pp. 1699-1709.

Bravo, R. H., 1991, Development of the Three-Dimensional Finite Analytic Method for Simulation of Fluid Flow and Conjugated Heat Transfer, Ph.D. Thesis, The University of Iowa.

Bravo, R. H., Sánchez, A., Chen, C. J., & Smith, T. F., [illegible] Convection and Radiation Heat Transfer Analysis in Three-Dimensional Arrays of Electronic Chips, Proc. of the [illegible] InterSociety Conference on Thermal Phenomena in Electronic Systems, Austin, pp. 149-154.

Chen, C. J., 1988, The Finite Analytic Method, in Handbook of Numerical Heat Transfer, ed. W. J. Minkowiz , E. M. Sparrow, G. E. Schneider, & R. H. Pletcher, Wiley, New York.

Fiveland, W. A., 1991, The Selection of Discrete Ordinate Quadrature Sets for Anisotropic Scattering, in Fundamentals of Radiation Heat Transfer, eds. W. A. Fiveland, A. L. Crosbie, A. M. Smith, and T. F. Smith, HTD-Vol. 160, A.S.M.E., pp. 89-96.

Jaluria, Y., 1985, Natural Convective Cooling of Electronic Equipment, in Natural Convection Fundamentals and Applications, ed. S. Kakac, W. Aung, & R. Viskanta, pp. 961-986.

Lee, S., & Yovanovich, M. M., 1989, Conjugate Heat Transfer from a Vertical Plate With Discrete Heat Sources under Natural Convection, ASME paper No. 89-WA/EEP-9.

Sánchez, A., Krajewski, W. F., & Smith, T. F., 1992, A General Purpose Radiative Transfer Model for Application to Remote Sensing in Multi-Dimensional Systems, IIHR Report No. 355, Iowa Institute of Hydraulic Research, The University of Iowa, Iowa City, Iowa

Sánchez, A. & Smith, T. F., 1992, Surface Radiation Exchange for Two-Dimensional Rectangular Enclosures Using the Discrete-Ordinates Method, J Heat Transfer, Vol. 114, No. 2, pp. 465-472

Shaw, H. J., Chen, W. L., & Chen, C. K., 1991, Study of the Laminar Mixed Convective Heat Transfer in Three-Dimensional Channel with a Thermal Source, J. of Electronic Packaging, Vol. 113, pp. 40-49

Smith, T. F., Beckermann, C., & Weber, S. W., 1991, Combined Conduction, Natural Convection, and Radiation Heat Transfer in an Electronic Chassis, J. of Electronic Packaging, Vol. 113, pp. 382-[illegible]

Sparrow, E. M., & Cess, R. D., 1978, Radiation Heat Transfer, Hemisphere Publishing, New York.

Sparrow, E. M., Niethammer, J. E., & Chaboki, A., 1982, Heat Transfer and Pressure Drop Characteristics of Rectangular Modules Encountered in Electronic Equipment, Int. J. Heat and Mass Transfer, Vol. 25, No. 7, pp. 961-973.